Growth of Carbon Nanotubes with Alkaline Earth Carbonate as Support

Arnaud Magrez,*,† Jin Won Seo,† Csilla Mikó,† Klára Hernádi,‡ and László Forró†

Institute of Physics of Complex Matter (IPMC), Ecole Polytechnique Fédérale de Lausanne, 1015 Lausanne, Switzerland, and Department of Applied and Environmental Chemistry, University of Szeged, 6720 Szeged, Rerrich B tér 1, Hungary

Received: January 20, 2005; In Final Form: April 4, 2005

Multiwalled carbon nanotubes (MWCNTs) were grown by chemical vapor deposition by applying C_2H_2 fluxed over $Fe_{1-x}Co_x$ catalyst supported by alkaline earth carbonate. Detailed investigations of the chemical process occurring prior and during the growth allowed us a significant improvement of the nanotube production rate and quality. We observed a strong influence of the catalyst stoichiometry on the carbon deposition rate and the nanotube characteristics. We also found evidence for the active role of the support in the growth process, which is explained by the decomposition of the carbonate at the growth temperature. Using the optimized parameters obtained from our study performed in a fixed bed furnace, we could improve the production rate to about 500 g/day of purified MWCNTs in our large-scale rotary tube furnace.

Introduction

Since the discovery of multiwalled carbon nanotubes (MWCNTs) in 1991,[1] numerous attempts have been made to synthesize them on a large scale and at low cost. Up to now, many different carbon nanotube (CNT) synthesis techniques have been used, for instance, arc discharge,[2] laser ablation,[3] catalytic chemical vapor deposition (CCVD),[4] flame synthesis,[5] and the solar energy route.[6] Among these techniques, the arc discharge and laser ablation methods often yield high-quality products; however, it is difficult to scale up these production methods. The CCVD method has become more popular and it is currently considered to be the most promising route for low-cost and large-scale synthesis of high-quality nanotube materials.

The CCVD synthesis method consists of the decomposition of a carbon-containing gas over a supported catalyst. Numerous catalysts[7−10] and carbon sources[7,11−14] have been tried out to improve the yield and the quality of CNT production. Improvement of CNTs quality has also been obtained by using different supports[7,15−17] or by inserting buffer layers between the catalyst and Si wafers for nanoelectronic applications.[18−20] Nevertheless, at this time, the relationship between the catalyst carrier and the nanotube characteristics is not well understood.

Very recently, we have shown that by using a rotary-tube furnace continuous production is possible; we obtained about 100 g/day of purified MWCNTs.[21] In this paper, we systematically study the influence of the catalyst composition, the nature of the support, the growth temperature, and the retention time of the catalyst in the furnace on the product yield and quality.

This parametric study has led to a catalyst composition very efficient for CNT growth and to the understanding of the role of the support material itself in the growth process. From this interpretation, and by optimizing parameters of the rotary-tube furnace (mainly temperature and rotation speed), we could scale up the rate to 500 g/day.

Experimental Section

MWCNTs were synthesized by CCVD of acetylene over $Fe_{1-x}Co_x$ catalysts supported by alkaline earth carbonates. In a typical catalyst preparation, a stoichiometric amount of metal salt—(cobalt(II) acetate tetrahydrate and/or iron(III) nitrate nonahydrate) corresponding to $Fe_{1-x}Co_x$ composition ($0 \leq x \leq 1$)—is dissolved in distilled water. MCO_3 (with M = Mg, Ca, Sr, Ba) is subsequently dispersed into the solution after neutralizing the latter with ammonia (necessary to avoid the release of CO_2 occurring when carbonates contact acids). The total concentration of metal is about 5 wt % relative to carbonate.[7,21] The resulting mixture is dried on a hot plate under continuous stirring. This brownish powder is referred to as "as-prepared catalyst" since it consists of a mixture of salts and carbonate, whereas "supported catalyst" is related to $Fe_{1-x}Co_x/MCO_3$ obtained after heat treatment of the as-prepared catalyst. Large batches of as-prepared catalyst are produced and kept in boxes without special care. For the production, 100 mg of the as-prepared catalyst is placed in an oven, flushed with nitrogen, and finally exposed to a mixture of acetylene and nitrogen (or argon), fluxed at 1 and 70 L/h, respectively.

The obtained samples were purified by 15 min of sonication in diluted hydrochloric acid (≈1 M). The resulting solid was filtered, washed with distilled water, and safely stored in ethanol. The term "mass of MWCNTs" used in this report corresponds to the material obtained by weighing the black material after the purification process and drying at 120 °C. During the purification metallic catalyst and support are dissolved in diluted hydrochloric acid.

Transmission electron microscopy (TEM) and scanning electron microscopy (SEM) were used to characterize the samples, in particular to differentiate the resulting materials characteristics, such as average diameter, level of purity, and wall structure. The TEM sample preparation involved dispersing the synthesized material in isopropyl alcohol by sonication, and a drop of suspension was put on a copper grid covered with holey carbon. For the TEM study Philips CM20 and CM300 microscopes were used for conventional and high-resolution mode operating at 200 and 300 kV, respectively. The latter was

* To whom any correspondence should be addressed. Fax: 00 41 (21) 693-4470. E-mail: arnaud.magrez@epfl.ch.
† Ecole Polytechnique Fédérale de Lausanne.
‡ University of Szeged.

10.1021/jp050363r CCC: $30.25
Published on Web 04/30/2005

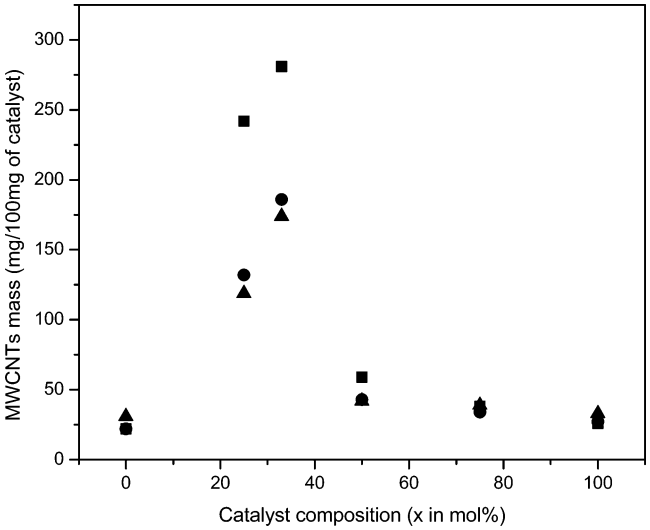

Figure 1. Evolution of the MWCNTs mass, after purification, with the composition x of the supported catalyst $Fe_{1-x}Co_x/CaCO_3$. CVD growth was performed for 30 min at 700 (■), 720 (●), 740 (▲).

equipped with a field-emission gun and a Gatan Image Filter (GIF 6000) for electron-energy loss spectroscopy (EELS) measurements. SEM micrographs were taken with a Philips XL 30 FEG operated at 30 kV.

X-ray powder diffraction experiments on catalyst particles were carried out with a Rigaku diffractometer in Bragg−Brentano geometry with monochromatic Cu Kα radiation. The data were collected in the $\theta-2\theta$ mode.

Thermogravimetry analysis (TGA) was carried out in nitrogen atmosphere (Derivatograph-Q, MOM) in order to characterize the temperature range of the $CaCO_3$ decomposition.

Results and Discussion

Optimization of the Parameters. First we performed a parametric study in a fixed-bed furnace in which a small quantity of catalyst was exposed to gases. Catalyst composition, support material, growth temperature, and retention time were optimized.

We first studied the influence of the catalyst composition $Fe_{1-x}Co_x$ on the carbon yield. In Figure 1, the evolution of the purified product mass is plotted versus the Co content (x), after 30 min at 700, 720, and 740 °C under C_2H_2/N_2 gas flux. For all three temperatures a clear dependence of the resulting yield on the catalyst composition is visible with the maximum yield at $x = 33$ mol % of cobalt. The highest maximum has been obtained at 700 °C. For almost all catalyst compositions, 700 °C yields the highest CNT amount. In particular, at $x = 33$ mol % the carbon-deposition rate is significantly sensitive to the temperature; from 700 °C an increase of 40 °C leads to a decrease of about 40% of the maximum yield. Hence, our observation clearly indicates that both the growth temperature and the catalyst composition have a strong influence on the yield. Furthermore, the resulting carbon content is higher for all binary alloys than for pure metals, in agreement with the earlier observation that nanoparticles of bimetallic alloys give higher yields of CNTs than monometallic catalysts.[22,23]

Figure 2a,b shows SEM images of purified CNTs grown at 700°C with $x = 33$ mol % catalyst. A dense mat of nanotubes can be seen with an outer diameter of about 15 nm and a length of a few microns without any indication of catalyst particles or amorphous carbon. As also confirmed by TEM (Figure 2c,d), the applied purification step allows a complete removal of the catalyst, thus samples with a high level of purity can be

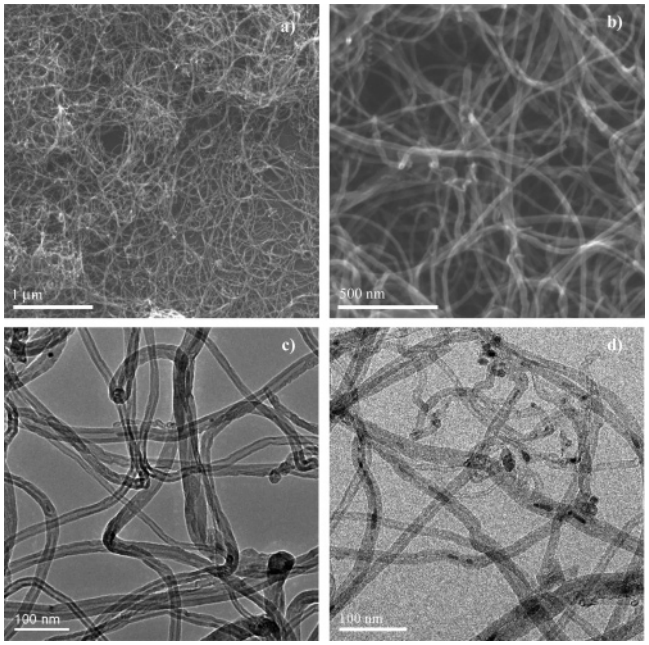

Figure 2. Electron microscopy studies. SEM pictures of purified MWCNTs obtained with Fe_2Co ($x = 33$ mol %) catalyst supported by $CaCO_3$ at 700 °C (a and b). TEM pictures of the product obtained at 700 °C with $x = 33$ mol % (c) and 100 mol % (d).

produced. Catalyst particles can only be found enclosed in CNTs, where they are not accessible by acid treatments.

A maximum yield of about 280 mg of purified MWCNTs was obtained from 100 mg of $x = 33$ mol % of as-prepared catalyst, at 700 °C. Flahaut et al.[24] obtained comparable results for the yield of single-walled CNT growth by using bimetallic $Fe_{1-x}Co_x$ catalyst. Unfortunately, they conclude the highest yield of carbon deposition for 25 mol % of Co without considering the 33 mol % composition.

To understand these results, we studied the structure of the catalyst particles at different stages of the nanotube growth. To this end, we performed X-ray Powder Diffraction (XRPD) on supported catalyst after annealing under (i) pure N_2 and (ii) N_2 mixed with acetylene, to identify their crystalline structure and their composition.[25] The most predominant phases present correspond to $CaCO_3$ and/or CaO; the fraction of the latter depends on the annealing atmosphere. Additional peaks are attributed to the most intense reflections of Fe_2CoO_4, CoO, or Fe_2Co depending on the stoichiometry or on the annealing atmosphere. The presence of a mixed Ca−Fe−Co oxide phase could not be confirmed, which indicates the absence of a reaction between $CaCO_3$ and Fe, Co precursor salts. To clarify the composition of the second phase formed in the metallic system depending on the stoichiometry $Fe_{1-x}Co_x$, we performed additional experiments with unsupported catalyst. For the preparation of the unsupported catalyst, we mixed the metallic salts in distilled water, without carbonate, and dried the solution under continuous stirring to preserve the homogeneity of the solution in the resulting solid. A few milligrams of these mixtures were introduced into the fixed-bed furnace and annealed. In Figure 3, the corresponding XRPD patterns are shown, which are consistent with the XRPD patterns of the supported catalyst except that the strong $CaCO_3$ and/or CaO peaks are missing and therefore easier to interpret. According to these measurements, after 10 min of annealing under N_2, a single-phase catalyst is obtained for 33 mol %, which corresponds to the spinel Fe_2CoO_4. A deviation from this composition leads to the presence of Fe_2O_3 ($x < 33$mol %) or CoO ($x >$

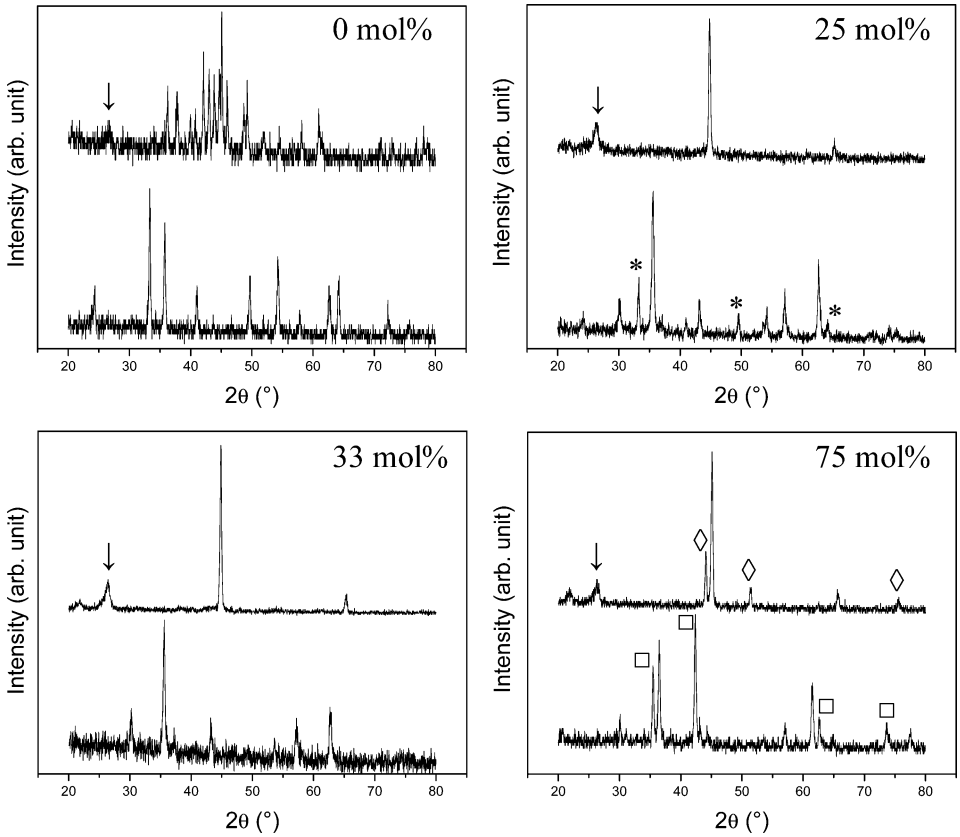

Figure 3. X-ray powder diffraction patterns. Both diagrams of the product after 10 min under N_2 (down) and after 10 min under N_2 plus 10 min of N_2/C_2H_2 (up) are presented for each composition. Arrows point to peaks related to graphitic carbon (3.4 Å) not as MWCNTs. For $x = 0$ mol %, patterns of Fe_2O_3 and Fe_3C were registered. For $x = 25$ mol %, an asterisk indicates Fe_2O_3 peaks. For $x = 33$ mol %, pure spinel Fe_2CoO_4 is obtained and produced afterward with acetylene Fe_2Co alloy mixed with carbon. For $x = 75$ mol %, CoO and Co impurities are identified with the symbols □ and ◇, respectively.

33mol %) impurities, respectively. After annealing 10 min under N_2 and an additional 10 min treatment under C_2H_2 mixed with N_2, XRPDs change drastically: For $x = 33\%$, the oxide is reduced and we obtain pure Fe_2Co alloy as expected. For lower Co concentration cementite Fe_3C is produced from the reaction of Fe_2O_3 and C_2H_2, while for the Co-rich compound CoO is predominantly formed under N_2, which reacts with acetylene to Co metal. The fact that the highest yield is obtained with the metal mixture that only forms Fe_2Co indicates that this alloy is the most active catalyst for CNT growth compared to Fe_3C or Co.

TEM analysis of CNTs after the purification step has shown a direct correlation between the catalyst composition and the density of embedded particles. Figure 2c shows a TEM image of CNTs grown from $x = 33$ mol % catalyst. Small embedded particles can only be seen rarely whereas for $x < 33$ and $x > 33$ mol % the density of the partial filling significantly increases. EELS was carried out on encapsulated particles present in a sample grown on $Fe_{0.75}Co_{0.25}$ catalyst (Figure 4b). No embedded particle with Fe_2Co composition was found. Most of the particles are iron rich with a small amount of Co. Detailed quantitative analysis revealed that the cobalt content is lower than 10%, which suggests a different phase than Fe_2Co. As derived from XRPD measurements, the catalyst of that composition forms a mixture of Fe_3C and Fe_2Co. Therefore we can conclude that the encapsulated particles predominantly originate from Fe_3C cementite doped with cobalt. For $x > 33$ mol %, catalyst forms Fe_2Co and Co. By increasing the cobalt content, the quantity of embedded Co particles increases. When $Co/CaCO_3$ is used, up to 80% of MWCNTs are partially filled (Figure 2d). Therefore, we assume that the lower catalytic activity of Fe_3C and Co compared to Fe_2Co originates from their tendency of being encapsulated in the nanotubes. The encapsulation reduces the surface contact of the Fe_3C or Co catalytic particles with acetylene. Therefore, this could be considered as a catalyst poisoning, which limits the CNT production.

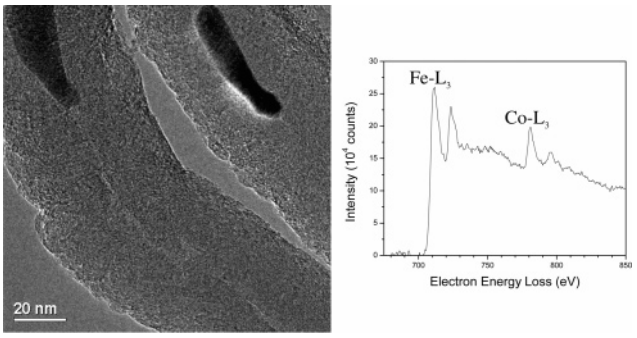

Figure 4. Electron energy loss spectroscopy. TEM picture (a) of an embedded particle in a nanotube-nanofilament grown with $x = 25$ mol % catalyst. The EELS spectrum (b) is leading to the $FeCo_{0.1(1)}$ metallic composition of the particle.

Another interesting feature of CNTs grown by using $CaCO_3$ support is the gas release during the purification process, which depends on the growth conditions. No noticeable release was observed when CNTs grown under the optimum yield conditions (100 mg of $x = 33$ mol % as-prepared catalyst, 700 °C, 30 min) were dispersed in the diluted acid while some deviations from these parameters lead to a significant gas release. Moreover, no gas release was observed when unsupported catalyst was used. Hence, the gas, identified as CO_2, is very likely a side product of the catalyst carrier $CaCO_3$, which

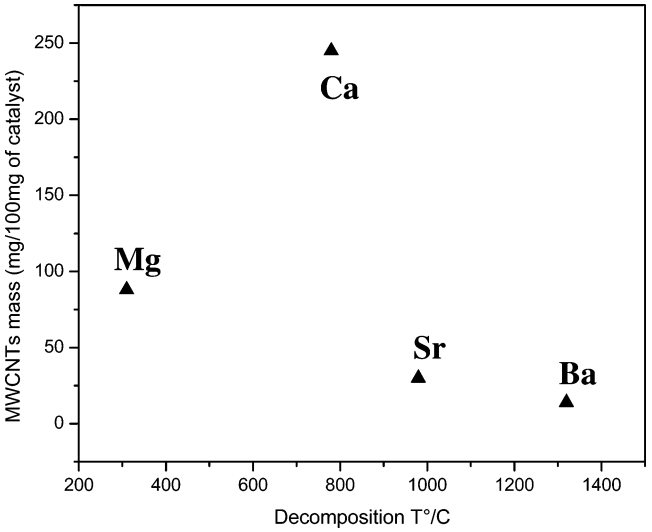

Figure 5. Evolution of the MWCNTs mass, after purification, versus the decomposition temperature of the support material (cation M of the carbonate MCO_3 is indicated) of $x = 25$ mol % catalyst after 30 min at 700 °C.

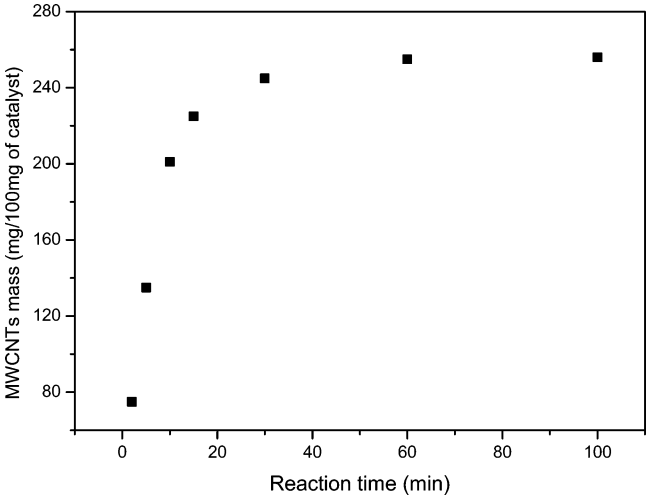

Figure 6. Evolution of the MWCNTs mass, after purification, versus the reaction time at 700 °C, using $CaCO_3$ as support for 100 mg of $x = 25$ mol % as-prepared catalyst.

decomposes into CaO and CO_2. Consequently, the presence of gas development during purification can directly be correlated with the decomposition state of $CaCO_3$ during the growth. When no gas is released during purification, the decomposition can be considered as fully taken place during the growth whereas the remaining $CaCO_3$ decomposes during the purification and leads to gas release. Since the amount of CO_2 released was found to strongly depend on the growth condition, we assume that the CO_2 groups originating from $CaCO_3$ decomposition also play a role in the growth of MWCNTs. When optimum parameters are used, CO_2 is completely consumed during the growth process (no release during purification). With a different catalyst composition than $x = 33$ mol %, CO_2 is not completely consumed during the growth and a CO_2 release is observed during the purification.

To substantiate any role of CO_2, we used other alkaline earth carbonates as support, and kept the optimum conditions for the growth. The plot of Figure 5 shows the evolution of the deposited carbon quantity versus the decomposition temperature of the carbonates ($MCO_3 \rightarrow MO + CO_2$). SEM confirmed the production of nanotubes for all samples and showed that the yield is higher when the working temperature of the furnace is closer to the decomposition temperature. The highest yield is obtained with $CaCO_3$, with a decomposition temperature (770 °C) closest to the CNT growth temperature (700 °C). For $MgCO_3$, since the growth temperature is much higher than the decomposition temperature, the support is completely transformed to the corresponding oxide (MgO). At the growth temperature, where acetylene is introduced, no CO_2 is present to take part in the growth process. For $SrCO_3$ and $BaCO_3$, the decomposition temperatures are substantially higher than the working temperature. Hence, CO_2 groups are strongly bonded and do not react with acetylene. Indeed a strong CO_2 release during the purification has been observed.

Moreover, TGA measurement has revealed the decomposition of $CaCO_3$ takes place between 600 and 810 °C. Therefore the quantity of CO_2 groups available for the carbon deposition is strongly temperature dependent in this range: when the temperature is raised from 700 to 740 °C the mass decreases from 92% to 78%, which corresponds to $CaO_{0.08}(CO_3)_{0.92}$ and $CaO_{0.22}(CO_3)_{0.78}$, respectively. Hence, the strong decrease of the CNT yield with the temperature as observed in Figure 1 can be explained by the thermal stability of $CaCO_3$: Increasing the growth temperature lowers the quantity of CO_2 compared to $CaCO_3$ and leads to a decrease of the carbon production. This observation also supports our interpretation that the decomposition of $CaCO_3$ plays an active role in the growth of CNTs.

The influence of the support materials on the final product of the CNT growth has already been observed,[26] but for the first time, we have proven that in the case of $CaCO_3$ the support acts as a source of chemical species involved in the growth. One can suppose that CO_2 reacts with acetylene to produce carbon for the MWCNTs via a few possible reactions between C_2H_2 and CO_2:

$$C_2H_2 + CO_2 \rightarrow 2C + CO + H_2O \quad (1)$$

$$C_2H_2 + CO_2 \rightarrow C + 2CO + H_2 \quad (2)$$

$$C_2H_2 + 2CO_2 \rightarrow 4CO + H_2 \quad (3)$$

$$C_2H_2 + 3CO_2 \rightarrow 5CO + H_2O \quad (4)$$

As these chemical processes suggested, carbon could directly be produced (reaction 1 and 2) or produced afterward as end products of reaction 2−4 via the disproportionation of carbon monoxide ($2CO \rightarrow C + CO_2$). Therefore, carbonates cannot be considered only as an inert support to avoid the coarsening of catalyst particles during the growth, which is generally interpreted as the role of the support material, but as an additional source of reactant for the synthesis.

Very recently, Hata et al.[27] have reported that the presence of oxygenated species in the reactor dramatically improves the CNT yield as observed in their study of the water vapor effect on the growth. Although the role of oxygenated species is not yet clear, this result is in agreement with our observations and indicates the importance of an additional oxygen source for the growth of CNTs.

Finally, we studied the carbon yield of the catalyst powder in the furnace versus the reaction time *t*. Figure 6 shows a saturation curve for the carbon deposit versus the reaction time. The first part of the reaction (2 to 30 min) is dominated by the growth of the CNTs. Within this growth time, no clear variation in the length or in the outer diameter of CNTs has been observed. This observation indicates that the growth kinetic of tubes is much faster than our shortest reaction time (2 min), in

agreement with the growth rate (1−50 μm per min) measured previously.[28,29] For $t > 30$ min, we assume that enough C_2H_2 was fluxed into the reactor so that all available catalytic particles and/or CO_2 groups from the carbonate were completely consumed.

A weight gain calculation is used to indicate the catalyst efficiency as the mass of CNTs produced relative to the weight of metal of the supported catalyst. This value, at saturation ($t > 30$ min), reaches 5100 g of MWCNTs per 100 g of Fe_2Co metal.

Large-Scale Production. From the previous parametric study, 100 mg of as-prepared Fe_2Co catalyst supported by $CaCO_3$ annealed for 30 min under C_2H_2/N_2 (fluxed at 1 and 70 L/h, respectively) were found as the optimum parameters. HRTEM observations have not shown drastic structural improvement of the CNTs at higher temperature but much less quantity, the 700 °C reaction temperature was therefore chosen for mass production. The procedure of CNTs preparation with the rotary tube furnace was extensively described in ref 21.

Obviously, some of the optimum parameters are strongly correlated: the gas flux and the retention time with the quantity of catalyst used. In our continuous production system, a larger quantity of powder is passing at the same time through the heated zone of the rotary tube. Therefore, we had to enrich the gas with acetylene and increase the retention time of the powder.

Calibration was performed to control the retention time. The influence of rotation speed and inclination of the quartz tube were checked. After several assays, they were set to 1 rpm and 15° (angle between the tube and the horizontal), respectively.

In our standard fixed-bed reactor, the semicontinuous production can yield up to 6.5 g/day of purified MWCNTs. With the rotary tube furnace technique, we achieved a continuous production rate of about 500 g/day of high-quality purified MWCNTs from 350 g of $Fe_2Co/CaCO_3$ catalyst passing through the heated zone in 24 h.

Conclusion

In this work we carried out a systematic study of the effect of catalyst composition, catalyst carrier, and retention time on the yield and quality of CNTs grown by CCVD. We identified Fe_2Co as the most active catalyst in the bimetallic family $Fe_{1-x}Co_x$. We found that metal salts deposited on the surface of the catalyst carrier decompose into oxides before being reduced to alloys. For $x = 33$ mol %, pure Fe_2CoO_4 is produced and forms Fe_2Co alloy by reaction with acetylene. Cobalt or iron enrichment of the as-prepared catalyst leads to the presence of Fe_3C or Co after exposure to acetylene. Their lower catalytic activity toward CNT growth was related to their encapsulation ability into carbon nanotubes.

After the composition optimization, we suggested an involvement of the CO_2 groups from carbonate in the CNT growth process. This was confirmed by using carbonates with different decomposition temperatures as catalyst support. $CaCO_3$ is the best support because of the good matching between the carbonate decomposition temperature and the nanotube growth. CO_2 groups originating from a carbonate react with acetylene to produce carbon for MWCNTs. A decrease of their quantity by raising the temperature from 700 to 740 °C leads to a drastic decrease of the yield of MWCNTs production.

With all these improvements, we obtained 280 mg of purified carbon nanotubes by using 100 mg of as-prepared catalyst. This yield corresponds to approximately 58% of the incoming acetylene being transformed to nanotubes, which is a remarkably high yield in the field. Applying the same parameters, we can produce 500 g/day of purified MWCNTs.

Acknowledgment. Authors want to thank R. Gaál for fruitful discussions. The authors also thank the TopNano21 program 5933.1, NCCR ''Nanoscale Science" of the Swiss National Science Foundation and the European Commission (NANOCOMP RTN network, HPRN-CT-2000-00037) for financing this investigation. Cs.M. thanks the Swiss National Science Foundation (NSF 61534) for a grant. K.H. thanks the National Science Foundation of Hungary (OTKA T046491) for financial support. We are also grateful to Centre Interdisciplinaire de Microscopie Electronique (CIME) at EPFL for access to electron microscopes as well as for technical support.

References and Notes

(1) Iijima, S. *Nature* **1991**, *354*, 56.
(2) Ebbesen, T. W.; Ajayan, P. M. *Nature* **1992**, *358*, 220.
(3) Thess, A.; Lee, R.; Smalley, R. E. *Science* **1996**, *273*, 483.
(4) Fan, S. S.; Chapline, M. G.; Franklin, N. R.; Tombler, T. W.; Cassell, A. M.; Dai, H. J. *Science* **1999**, *283*, 512.
(5) Vander Wal, R. L.; Ticich, T. M. *Chem. Phys. Lett.* **2000**, *323*, 217.
(6) Laplaze, D.; Bernier, P.; Maser, W. K.; Flamant, G.; Guillard, T.; Loiseau, A. *Carbon* **1998**, *36*, 685.
(7) Seo, J. W.; Couteau, E.; Umek, P.; Hernadi, K.; Marcoux, P.; Lukic, B.; Forro, L. *New J. Phys.* **2003**, *5*, 120.1.
(8) Li, Y.; Liu, J.; Wang, Y. Q.; Wang, Z. L. *Chem. Mater.* **2001**, *13*, 1008.
(9) Che, G.; Lakshmi, B. B.; Martin, C. R.; Fisher, E. R.; Ruoff, R. S. *Chem. Mater.* **1998**, *10*, 260.
(10) Ren, Z. H.; Huang, Z. P.; Wang, D. Z.; Wen, J. G.; Xu J. W.; Wang, J. H. *Appl. Phys. Lett.* **1999**, *75*, 1086.
(11) Cassell, A. M.; Raymakers, J. A.; Kong J.; Dai, H. J. *J. Phys. Chem. B* **1999**, *103*, 6484.
(12) Kong, J. A.; Cassell, A. M.; Dai, H. J. *Chem. Phys. Lett.* **1998**, *292*, 567.
(13) Dai, H. J.; Rinzler, A. G.; Nikolaev, P.; Thess, A.; Colbert, D. T.; Smalley, R. E. *Chem. Phys. Lett.* **1996**, *260*, 471.
(14) Bronikowski, M. J.; Willis, P. A.; Colbert, D. T.; Smith, K. A.; Smalley, R. E. *J. Vac. Sci. Technol. A* **2001**, *19*, 1800.
(15) Hernadi, K.; Fonseca, A.; Piedigrosso, P.; Delvaux, M.; Nagy, J. B.; Bernaerts, D. *Catal. Lett.* **1997**, *48*, 229.
(16) Hernadi, K.; Fonseca, A.; Nagy, J. B.; Bernaerts, D.; Fudala, A.; Lucas, A. A. *Zeolites* **1996**, *17*, 416.
(17) Nagaraju, N.; Fonseca, A.; Konya, Z.; Nagy, J. B. *J. Mol. Catal. A* **2002**, *181*, 57−62.
(18) de los Arcos, T.;. Garnier, M. G.; Seo, J. W.; Oelhafen, P.; Mathys, D.; Thonmen, V. *J. Phys. Chem. B* **2004**, *108*, 7728.
(19) Delzeit, L.; Chen, B.; Cassell, A. M.; Stevens, R.; Nguyen, C.; Meyyappan, M. *Chem. Phys. Lett.* **2001**, *348*, 368−74.
(20) Delzeit, L.; McAninch, I.; Cruden, B. A.; Hash, D.; Chen, B.; Han, J. *J. Appl. Phys.* **2002**, *91*, 6027−33.
(21) Couteau, E.; Hernadi, K.; Seo, J. W.; Thiên-Nga, L.; Miko, Cs.; Gaal, R.; Forro, L. *Chem. Phys. Lett.* **2003**, *378*, 9.
(22) Guo, T.; Nikolaev, P.; Thess, A.; Colbert, D. T.; Smalley, R. E. *Chem. Phys. Lett.* **1995**, *243*, 49.
(23) Kiang, C. H.; Goddard, W. A., III *Phys. Rev. Lett.* **1996**, *76*, 2515.
(24) Flahaut, E.; Govindaraj, A.; Peigney, A.; Laurant, Ch.; Rousset, A.; Rao, C. N. R. *Chem. Phys. Lett.* **1999**, *300*, 236.
(25) Emmenegger, C.; Bonard, J. M.; Mauron, O.; Sudan, P.; Lepora, A.; Grobety, B.; *Carbon* **2003**, *41*, 539.
(26) de los Arcos, T.; Garnier, M. G.; Oelhafen, P.; Mathys, D.; Seo, J. W.; Domingo, C. *Carbon* **2004**, *42*, 187.
(27) Hata, K.; Futaba, D. N.; Mizuno, K.; Namai, T.; Yumura, M.; Iijima, S. *Science* **2004**, *306*, 1362.
(28) Bonard, J. M.; Croci, M.; Conus, F.; Stockli, T.; Chatelain, A. *Appl. Phys. Lett.* **2002**, *81*, 2836.
(29) Geohegan, D. B.; Puretzky, A. A.; Ivanov, N. N.; Jesse, S.; Fres, G.; Howe, J. Y. *Appl. Phys. Lett.* **2003**, *83*, 1851.